Application of the Rigid Finite Element Method to the Simulation of Cable-Driven Parallel Robots

Philipp Tempel[1]([✉]), Andreas Schmidt[2], Bernard Haasdonk[2], and Andreas Pott[1]

[1] Institute for Control Engineering of Machine Tools and Manufacturing Units (ISW), University of Stuttgart, Seidenstr. 36, 70174 Stuttgart, Germany
{philipp.tempel,andreas.pott}@isw.uni-stuttgart.de
[2] Institute for Applied Analysis and Numerical Simulation (IANS), University of Stuttgart, Pfaffenwaldring 57, 70569 Stuttgart, Germany
{andreas.schmidt,bernard.haasdonk}@mathematik.uni-stuttgart.de

Abstract. Kinematics and dynamics of cable-driven parallel robots are affected by the cables used as force and motion transmitting elements. Flexural rigidity of these cables is of major interest to better understand dynamics of these systems and to improve their accuracy. The approach for modeling spatial cable dynamics, as presented in this paper, is based on the modified rigid-finite element method using rigid bodies and spring-damper elements. With this, a simulation of a planar 3 degrees of freedom cable-driven parallel robot is constructed as a multi-body dynamics model. Under consideration of holonomic constraints and Baumgarte stabilization, a simulation framework for the simulation of cable-driven parallel robots including dynamics of the cables is developed and presented.

Keywords: Parallel kinematics · Multi-body dynamics · Flexible joints · Holonomic systems · Model order reduction

1 Introduction

Cable-driven mechanisms have been known for thousands of years starting in ancient Egypt and reaching all the way till modern centuries. Such systems, like mooring, supporting, or lifting devices in offshore engineering, cable-suspension bridges, or cranes are very likely known to the reader. Another field of application comes from replacing rigid links usually found in Gough-Stewart platforms (see Fig. 1a) with cables, yielding a cable-driven parallel robots (shortened cable robot, see Fig. 1b). This enables such systems to outperform their rigid-link counterparts by magnitudes when it comes to dynamics, workspace, or payload. On the downside, these benefits come at a cost stemming from the use of flexible links as force and motion transmitting elements as these introduce unilateral

(a) CAD rendering of a Gough-Stewart platform, a general hexapod with 6 degrees of freedom and 6 actuators.
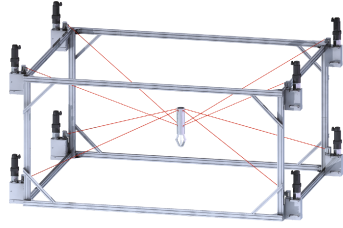
(b) Representation of a general cable robot with 6 degrees of freedom and 8 actuators (cables).

Fig. 1. Comparative display of a general Gough-Stewart platform (a) and a cable robot (b).

constraints into the system: cables can only exert tensile forces i.e., can only pull. Additionally, their resistance to transversal forces i.e., perpendicular to the cable's neutral axis, is negligible. This effect is very prominent when jerky motions or sharp changes in the direction of motion along a trajectory occur.

Industrial application of the cable robot technology was first studied by Albus et al. for the NIST RoboCrane [2]. To foster research, cables were assumed ideal i.e., to be forming a straight line between two points without any longitudinal flexibility or inherent dynamics. However, mechanical properties of cables differ from rigid links thus modeling of cables was further extended. Besides considering cable longitudinal flexibility by means of linear [10] or non-linear models [5,8], the dynamics were researched in only very limited extend. In [7], the authors employed XDE to simulate cable robots with discretized cables allowing for coiling, yet the Reissner beam for cable modeling with a resolution of 0.02 m makes for very slow simulation and induced oscillations. The cable robot analysis and simulation framework CASPR [6] provides tools for designing cable robots, yet simulation also allows for only state of the art cable models. A multi-body approach for large-span suspended cable robots was introduced in [3], neglecting extensibility of the cables as well as bending stiffness, yet the authors explicitly consider winding of the cables.

In this contribution, the well-established finite element discretization method for cables based on the modified rigid finite element method derived by [1], accounting for both bending and longitudinal flexibility, is applied to simulation of cable robots. The model is extended such that it allows for attaching multiple cables to arbitrary points on a rigid body that is assumed to represent the mobile platform of cable robots. To account for expensive evaluation of the extended system dynamics, model order reduction techniques are further employed reducing the computational complexity and enabling efficient simulation of the system.

The structure of this paper is as follows: in Sect. 2, the model of a single cable is derived as well as the synthesis for a multi-cable setup including the cable robot mobile platform is shown. Analysis of the model is performed and numerical results are given, including application of model order reduction techniques since calculation of the equation dynamics is time-consuming. After a

discussion of the combined model in Sect. 3 highlighting its applicability to simulation of cable robots, a conclusion is drawn in Sect. 4 also pointing out further steps to improving the model.

2   Model Synthesis and Analysis

In this section, we derive the dynamics of the system used for simulation of a cable robot. The model is based on the modified rigid finite element approached presented by Adamiec–Wójcik et al. [1]. Since our coordinate system and notation differ and due to the importance of several components to the work presented here, we will briefly reproduce the derivation.
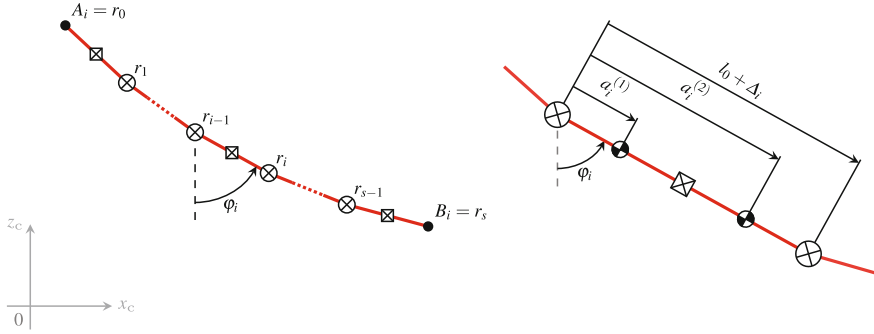
(a) Division of the cable into s segments interconnected with radial spring and damper elements inbetween.

(b) Segment of the cable modeled as rigid finite element (rfe) in a deformed state.

Fig. 2. Planar cable model used with division of the cable (a) into s segments composed of two rfes adjoined through linear sde shown in (b).

2.1   Cable Dynamics

We assume a planar cable model as shown in Fig. 2 comprised of stretching and bending stiffness. The cable is fixed at A_i and split into s rigid finite elements (rfes) with generalized coordinates strain Δ_i and angle φ_i in $\boldsymbol{q}_i = [\Delta_i, \varphi_i]^\mathsf{T}$. Each segment, denoted with $^{(1)}$ and $^{(2)}$, is composed of two rigid bodies of mass m_i and moment of inertia J_i connected via a linear spring-damper element (sde). The full system state is

$$\boldsymbol{q} = \left[\Delta_1, \varphi_1, \Delta_2, \varphi_2, \ldots, \Delta_s, \varphi_s\right]^\mathsf{T} = \left[\boldsymbol{q}_1^\mathsf{T}, \boldsymbol{q}_2^\mathsf{T}, \ldots, \boldsymbol{q}_s^\mathsf{T}\right]^\mathsf{T}. \tag{1}$$

The coordinate of each rfe segment can be readily derived to read

$$\boldsymbol{r}_i = \boldsymbol{r}_0 + \sum_{k=1}^{i} (l_0 + \Delta_k) \begin{bmatrix} \sin \varphi_k \\ -\cos \varphi_k \end{bmatrix}, \quad i = 1, \ldots, s, \tag{2}$$

where $l_0 = L/s$ is the unstrained length of each segment. Furthermore, the position of the distal point of the cable is to be given by $\boldsymbol{r}_{\mathrm{end}}(t)$, which translates to the holonomic constraint $\boldsymbol{\Phi}(t) \equiv 0$ with

$$0 \equiv \boldsymbol{\Phi}(t) = \boldsymbol{r}_s(t) - \boldsymbol{r}_{\text{end}}(t) \quad t \geq 0. \tag{3}$$

The governing system dynamics are established through Lagrangian mechanics

$$\frac{\mathrm{d}}{\mathrm{d}t} \frac{\partial \mathscr{L}}{\partial \dot{q}_i} - \frac{\partial \mathscr{L}}{\partial q_i} + \sum_{j=1}^{c} \lambda_j \frac{\partial \boldsymbol{\Phi}_j}{\partial q_i} = \frac{\partial P}{\partial \dot{q}_i} + \sum_{j=1}^{s} \boldsymbol{F}_j \cdot \frac{\partial \boldsymbol{r}_j}{\partial q_i}, \quad i = 1, \ldots, 2s \tag{4}$$

in which $\mathscr{L} = \sum_{i=1}^{s} T_i - U_i$ is the Lagrangian, $\boldsymbol{\Phi}_j$ is the jth component of the geometric constraints vector from Eq. (3) (in planar case $c \equiv 2$) and λ_j are Lagrange multipliers. Additional external forces $\boldsymbol{F}_j = [F_{j,\text{x}}, F_{j,\text{z}}]^{\mathsf{T}}$ at the massless sde $\boldsymbol{r}_j$ (cf. Eq. (2)) are also considered. Kinetic energies T_i, potential energies U_i, and dissipative energies P_i of the ith segment are

$$T_i = \frac{m_i}{2} \left(\|\dot{\boldsymbol{r}}_i^{(1)}\|^2 + \|\dot{\boldsymbol{r}}_i^{(2)}\|^2 \right) + \frac{1}{2} \left(J_i^{(1)} + J_i^{(2)} \right) \dot{\varphi}_i^2, \tag{5a}$$

$$U_i = \frac{c_{\text{L}}}{2} \Delta_i^2 + \frac{c_{\text{R}}}{2} (\varphi_i - \varphi_{i-1})^2 + m_i g \left(\boldsymbol{r}_{i,\text{z}}^{(1)} + \boldsymbol{r}_{i,\text{z}}^{(2)} \right), \tag{5b}$$

$$P_i = \frac{d_{\text{L}}}{2} \dot{\Delta}_i^2 + \frac{d_{\text{R}}}{2} (\dot{\varphi}_i - \dot{\varphi}_{i-1})^2, \tag{5c}$$

considering spring and damper elements with respective linear and angular spring coefficients c_{L}, c_{R}, and linear and angular damper coefficients d_{L} and d_{R}, respectively.

The system dynamics can be described through the index-3 differential algebraic equation system

$$\boldsymbol{M}(t, \boldsymbol{q}, \dot{\boldsymbol{q}}) \cdot \ddot{\boldsymbol{q}} = \boldsymbol{f}(t, \boldsymbol{q}, \dot{\boldsymbol{q}}) + \boldsymbol{B}(t, \boldsymbol{q}, \dot{\boldsymbol{q}}) \cdot \boldsymbol{F}(t) - \boldsymbol{\Phi}_{\boldsymbol{q}}(t, \boldsymbol{q})^{\mathsf{T}} \cdot \boldsymbol{\lambda}, \quad 0 = \boldsymbol{\Phi}(t, \boldsymbol{q}). \tag{6}$$

Stable numerical simulations without induced drift requires index reduction to receive an index-1 system, which is achieved by applying Baumgarte stabilization technique (compare [4]):

$$\begin{bmatrix} \boldsymbol{M} & \boldsymbol{\Phi}_{\boldsymbol{q}}^{\mathsf{T}} \\ \boldsymbol{\Phi}_{\boldsymbol{q}} & 0 \end{bmatrix} \begin{bmatrix} \ddot{\boldsymbol{q}} \\ \boldsymbol{\lambda} \end{bmatrix} = \begin{bmatrix} \boldsymbol{f} + \boldsymbol{B} \cdot \boldsymbol{F} \\ \boldsymbol{\gamma} - 2\alpha\dot{\boldsymbol{\Phi}} - \beta^2 \boldsymbol{\Phi} \end{bmatrix}, \quad \boldsymbol{\gamma} \equiv -(\boldsymbol{\Phi}_{\boldsymbol{q}}\dot{\boldsymbol{q}})_{\boldsymbol{q}}\dot{\boldsymbol{q}} - 2\boldsymbol{\Phi}_{\boldsymbol{q}t}\dot{\boldsymbol{q}} - \ddot{\boldsymbol{\Phi}} \tag{7}$$

2.2 Multi-cable Dynamics with Platform

We extend the model derived in Sect. 2.1 such that it is applicable to simulation of cable robots consisting of a platform and m cables. To begin with, we assume the platform to be of rectangular shape with width and height w and h, respectively, mass m_{P}, and moment of inertia J_{P}. The platform can be described by the generalized coordinates $\boldsymbol{q}_{\text{p}} = [x_{\text{p}}, z_{\text{p}}, \Theta_{\text{p}}]^{\mathsf{T}}$ with Cartesian position $\boldsymbol{r}_{\text{p}} = [x_{\text{p}}, z_{\text{p}}]^{\mathsf{T}}$ and angle of rotation Θ_{p}. Further stating the cables are attached to the platform at the cable attachment points $\boldsymbol{b}_i$ w.r.t. the platform's coordinate system, the holonomic constraints according to Eq. (3) for the distal point of the ith cable $\boldsymbol{r}_{i,\text{end}}(t)$ and the cable attachment point on the platform $\boldsymbol{r}_{b_i}(t)$ yield

$$\boldsymbol{r}_{\text{end}}^{(i)}(t) = \boldsymbol{r}_{\text{p}}(t) + \boldsymbol{R}\boldsymbol{b}_i, \qquad \boldsymbol{r}_{b_i}(t) = \boldsymbol{r}_s^{(i)}(t). \tag{8}$$

where $\boldsymbol{R} = \boldsymbol{R}(\Theta_{\mathrm{p}})$ is the rotation matrix for the current platform rotation. The dynamics of the platform can be easily derived from Lagrangian mechanics under consideration of holonomic constraints similar to Eqs. (4) and (7), respectively.

2.3   Model Order Reduction

The nonlinear DAE system Eq. (7) contains functions that are costly to evaluate. This is due to the complex trigonometric couplings and interactions within all nodes in the system. The overall computational demands might thus be too high to allow for efficient simulations. Model order reduction (MOR) techniques can help to overcome the above mentioned limitations by replacing the computationally expensive model with cheap yet accurate surrogates. For this purpose we employ the so-called trajectory-piecewise-linear approach (TPWL-approach), which was first introduced in [9]. By using this technique, the complex non-linear functions are replaced by a weighted linear combination of linearizations around several well-chosen points in the state space: We hence choose a set of linearization points $\{\bar{t}_i, \bar{\boldsymbol{q}}_i\}_{i \in I}$ for a preferably small set $I = \{1, \ldots, N_I\}$, and replace the non-linear functions by linearizations of the following form:

$$\boldsymbol{f}(t, \boldsymbol{q}, \dot{\boldsymbol{q}}) \approx \sum_{i \in I} \omega_i(\boldsymbol{q}) \left(\boldsymbol{f}(\bar{t}_i, \bar{\boldsymbol{q}}_i, \dot{\bar{\boldsymbol{q}}}_i) + D\boldsymbol{f}(\bar{t}_i, \bar{\boldsymbol{q}}_i, \dot{\bar{\boldsymbol{q}}}_i)(\boldsymbol{q} - \bar{\boldsymbol{q}}_i) \right). \tag{9}$$

The weightings $\omega_i(\boldsymbol{q})$ are chosen in such a way that $\sum_{i \in I} \omega_i(\boldsymbol{q}) = 1$ and are calculated in order to switch and interpolate between the linearized models, depending on where in the state space the simulation currently is located. More sophisticated techniques and dimension reduction via projection can furthermore yield significant speedups as discussed in [9]. In our case, we apply the TPWL approach to the equations for $\boldsymbol{f}$ only, and keep the nonlinear holonomic constraint equations to guarantee that the cables are correctly linked.

3   Discussion

For numerical simulation, we choose two cables with length $L_0 = 3\,\mathrm{m}$ and a platform of size $1\,\mathrm{m} \times 0.3\,\mathrm{m}$. The cables are suspended at $\boldsymbol{r}_0^{(1)} = [0, 0]^{\mathsf{T}}$ and $\boldsymbol{r}_0^{(2)} = [1, -0.25]^{\mathsf{T}}$ and are attached at $\boldsymbol{b}_1 = [-0.5, 0.15]^{\mathsf{T}}\,\mathrm{m}$ and $\boldsymbol{b}_2 = [0.5, 0.15]^{\mathsf{T}}\,\mathrm{m}$, respectively. We choose $s = 20$ segments for the discretization of either cable, resulting in a DAE system of dimension 170, including the algebraic equations and Lagrange multipliers. All functions in the DAE formulation from Eq. (6) are derived analytically by utilizing the symbolic calculation techniques of MAPLE, and are then exported to optimized MATLAB functions. The resulting DAE system is solved by using MATLAB's builtin `ode15s` solver with default accuracy.

As a test case, we simulate the system for $T = 15\,\mathrm{s}$, where we apply a time-dependent force on the center of the platform as depicted in Fig. 3. With this setup we aim to investigate the transition of the cables from tensed to non-tensed and back to tensed state. For such, the external force on the platform is applied in
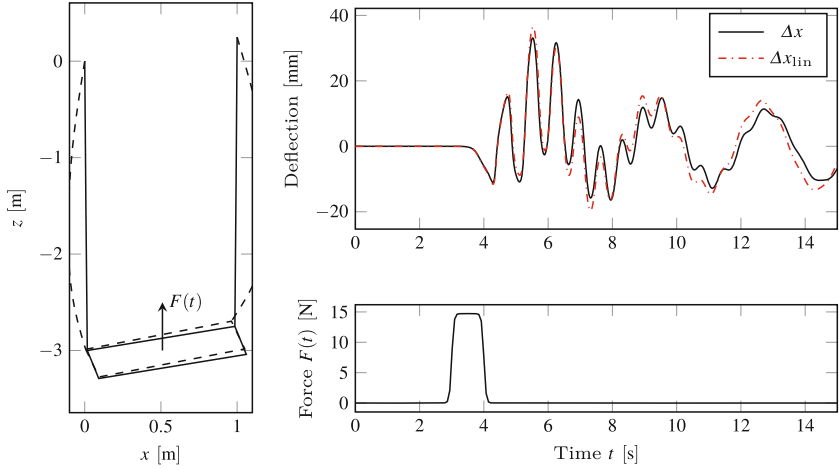
Fig. 3. The simulation setting for our experiments (left). The solid line shows the system at $t = 0\,\mathrm{s}$, the dashed line at $t = 4.3\,\mathrm{s}$. The right plots show the x-deflection of the platform (top) for the full (Δx) and linearized (Δx_{lin}) simulations, as well as the applied external force (bottom).

the positive z-direction i.e., negative direction of gravity to make the cables slack. During increasing force, the platform is being pushed up and the cables go slack. With the external force decreasing, the cables get tensed again yet apply different forces onto the platform. Comparing this behavior with the standard cable model of straight lines, the platform's bouncing motion looks more realistically since the flexural rigidity of the cables is no explicitly considered.

The simulation was run with the full non-linear model and took $39.1\,\mathrm{s}$. By using the proposed TPWL-approach for $\boldsymbol{f}$ only, where we choose the initial configuration and the true solution at times $t \in \{4.2\,\mathrm{s}, 5\,\mathrm{s}, 5.5\,\mathrm{s}\}$ as linearization points, we can simulate the system in $20\,\mathrm{s}$ and thus gain almost 53% speedup while making a relative error of only 4.1%, measured in the space-time norm $\|\boldsymbol{q}\| := \left(\int_0^T \|\boldsymbol{q}(t)\|^2 \, \mathrm{d}t\right)^{1/2}$. Automatic techniques for the choice of the linearization points and projection-based MOR techniques yield more accurate and efficient results.

4   Conclusions

A cable model based on the modified rigid finite element method, as presented in this paper, shows reasonable results for the motion of the cables and the platform. Using the approach given in this work, cables can be attached to a rigid body representing the mobile platform. Due to the time-consuming evaluation of the system dynamics, advanced mathematical techniques are employed to accelerate the calculations. A combination of the proposed linearization ansatz and a projection-based technique will lead to even larger speed-ups.

Currently, the dynamics of the platform can only be simulated very limitedly, despite the model allowing for additional dynamics of the platform to simulate cable robots with up to 6 degrees of freedom and additional cables. To further improve numerical results, the mechanical properties of the cable need to be more closely obtained. As is known by related contributions, elasticity of the used fiber cables is non-linear thus applying Hooke's law for tension may not be accurate enough. Additionally, initial investigations make assuming a progressive bending stiffness of the cable with very small resistance more accurate. With the modularity of the model, all of these approaches can easily be integrated in the presented simulation framework and thus will be investigated in future work.

References

1. Adamiec-Wójcik, I., Awrejcewicz, J., Brzozowska, L., Drg, L.: Modelling of ropes with consideration of large deformations and friction by means of the rigid finite element method. In: Awrejcewicz, J. (ed.) Applied Non-Linear Dynamical Systems. Springer Proceedings in Mathematics & Statistics, vol. 93, pp. 115–137. Springer International Publishing, Cham (2014). doi:10.1007/978-3-319-08266-0_9

2. Albus, J.S., Bostelman, R.V., Dagalakis, N.G.: The NIST RoboCrane. J. Res. Nat. Inst. Stand. Technol. **97**, 373–385 (1992)

3. Collard, J.F., Lamaury, J., Gouttefarde, M.: Dynamics modelling of large suspended parallel cable-driven robots. In: 2011 ECCOMAS Thematic Conference on Multibody Dynamics, pp. 1–13 (2011)

4. Flores, P., Pereira, R., Machado, M., Seabra, E.: Investigation on the Baumgarte stabilization method for dynamic analysis of constrained multibody systems. In: Ceccarelli, M. (ed.) Proceedings of EUCOMES 2008, pp. 305–312. Springer, Dordrecht (2008). doi:10.1007/978-1-4020-8915-2_37

5. Kozak, K., Zhou, Q., Wang, J.: Static analysis of cable-driven manipulators with non-negligible cable mass. In: IEEE Conference on Robotics, Automation and Mechatronics, vol. 2, pp. 886–891 (2004). doi:10.1109/RAMECH.2004.1438035

6. Lau, D., Eden, J., Tan, Y., Oetomo, D.: CASPR: a comprehensive cable-robot analysis and simulation platform for the research of cable-driven parallel robots. In: 2016 IEEE/RSJ International Conference on Intelligent Robots and Systems (IROS), pp. 3004–3011 (2016). doi:10.1109/IROS.2016.7759465

7. Michelin, M., Baradat, C., Nguyen, D.Q., Gouttefarde, M.: Simulation and control with XDE and Matlab/Simulink of a cable-driven parallel robot (CoGiRo). In: Pott, A., Bruckmann, T. (eds.) Cable-Driven Parallel Robots. Mechanisms and Machine Science, vol. 32, pp. 71–83. Springer International Publishing, Cham (2015). doi:10.1007/978-3-319-09489-2_6

8. Miermeister, P., Kraus, W., Lan, T., Pott, A.: An elastic cable model for cable-driven parallel robots including hysteresis effects. In: Pott, A., Bruckmann, T. (eds.) Cable-Driven Parallel Robots. Mechanisms and Machine Science, vol. 32, pp. 17–28. Springer International Publishing, Cham (2015). doi:10.1007/978-3-319-09489-2_2

9. Rewieśki, M., White, J.: A trajectory piecewise-linear approach to model order reduction and fast simulation of nonlinear circuits and micromachined devices. In: Proceedings of the 2001 IEEE/ACM International Conference on Computer-Aided Design, pp. 252–257. IEEE Press (2001)
10. Verhoeven, R.: Analysis of the workspace of tendon-based Stewart platforms. Ph.D. Thesis. Universität Duisburg-Essen, Duisburg, Germany (2004)